Indonesian Journal of Electrical Engineering and Computer Science
Vol. 25, No. 2, February 2022, pp. 721~731
ISSN: 2502-4752, DOI: 10.11591/ijeecs.v25.i2.pp721-731

Topology network effects for double synchronized switch harvesting circuit on vibration energy harvesting

Youssef El Hmamsy[1], Chouaib Ennawaoui[1], Abdelowahed Hajjaji[1,2]
[1]Laboratory of Engineering Sciences for Energy (LabSIPE), National School of Applied Sciences, Chouaib Doukkali University, El Jadida, Morocco
[2]The Higher School of Education and Formation, Chouaib Doukkali University, El Jadida, Morocco

Article Info

Article history:

Received Jul 7, 2021
Revised Nov 21, 2021
Accepted Dec 6, 2021

Keywords:

Double synchronized switch harvesting
Energy harvesting
Network topology
Piezoelectric

ABSTRACT

Energy extraction takes place using several different technologies, depending on the type of energy and how it is used. The objective of this paper is to study topology influence for a smart network based on piezoelectric materials using the double synchronized switch harvesting (DSSH). In this work, has been presented network topology for circuit DSSH (DSSH Standard, Independent DSSH, DSSH in parallel, mono DSSH, and DSSH in series). Using simulation-based on a structure with embedded piezoelectric system harvesters, then compare different topology of circuit DSSH for knowledge is how to connect the circuit DSSH together and how to implement accurately this circuit strategy for maximizing the total output power. The network topology DSSH extracted power a technique allows again up to in terms of maximal power output compared with network topology standard extracted at the resonant frequency. The simulation results show that by using the same input parameters the maximum efficiency for topology DSSH in parallel produces 120% more energy than topology DSSH-series. In addition, the energy harvesting by mono-DSSH is more than DSSH-series by 650% and it has exceeded DSSH-ind by 240%.

Corresponding Author:

Youssef El Hmamsy
Laboratory of Engineering Sciences for Energy (LabSIPE)
National School of Applied Sciences, Chouaib Doukkali University
El Jadida, Morocco
Email: elhmamsyyoussef@gmail.com

1. INTRODUCTION

In the past few years, piezoelectric micro-generators whose energy is derived from ambient vibration have a promising future in applications such as self-powering of abandoned sensor networks because of good electro-mechanical conversion performance and compatibility with the microsystem manufacturing technologies. Using the energy harvested from the ambient environment to power the electronic devices can avoid environmental pollution and battery replacement problems.

Today constitute a new field of application, which lies between mechanics and electronics, for example the generation of ultrasound with sonar, transducers to medical use (ultrasound), positioning (actuators and motors), gas lighters or fuel injectors (direct injection in diesel engines). Guyomar *et al*. [1] proposed the most basic circuit topology synchronized switch harvesting on inductor (SSHI). This approach allows to improve of the coupling coefficient of the electromechanical system using piezoelectric materials. It saves up to 10 times in terms of recovered energy. The technique is derived from the synchronized switch damping (SSD) semi-passive vibration damping technique. There are two configurations, parallel SSHI and serial SSHI. When the vibration of the vibrating structure represented by the piezoelectric transducer is at its maximum, the switch closes. The internal capacitance and inductance constitute an oscillator circuit whose frequency must be chosen smaller than the mechanical vibration frequency so that the resonant circuit will almost instantaneously reverse the voltage of the piezoelectric element and thus bring the vibration speed and the generated voltage into phase.

Mistral *et al.* [2] compared the s-SSHI circuit, the p-SSHI circuit, and the standard circuit under various operating frequency conditions. In the average coupling state (k2QM=1), the optimum resonance frequency for p-SSHI is around the short-circuit frequency, the optimum resonance for s-SSHI is around the open circuit frequency. However, with the same configuration, the standard alternating current (AC) circuit has two maximums at a short-circuit frequency and at an open circuit frequency. Nevertheless, in long-term operation, the property of the harvester (the resonance frequency) may be a change in temperature or humidity, which leads to degradation of the optimum impedance of the frequency adaptation. A load-independent processing circuit such as Lefeuvre *et al.* [3], proposed synchronous electric charge extraction (SECE) can avoid these problems. In general, the power harvested with SECE is 4 times higher than the standard technique and is completely independent of the load. The main problem of SECE is the switch on-time tuning for perfect voltage cancellation. This time may change with the piezoelectric material capacitance (temperature, stress, or stain amplitude). The research proposed an optimized version of SECE, called optimized synchronous electric charge extraction (OSECE) [4]-[5]. Can be considered as a hybrid between SECE (for low load impedance) and SSHI (for high load impedance). Transformer replaces the diode bridge with two primary windings connected to the piezo element with two opposing unidirectional switching cells triggered on maximum and minimum voltage respectively.

The normal topology of all synchronized switch harvesting (SSH) circuits including double synchronized switch harvesting (DSSH) [6] enhanced synchronized switch harvesting (ESSH) [7]-[8]. The enhanced synchronized switch harvesting (ESSH) configuration is actually an improvement of the DSSH technique. The ESSH technique depends on the Cint intermediate capacitor does not discharge completely through the inductor. This amount of energy stored in Cint ensures a better compromise in switching timing between the extracted energy and vibration damping. In addition to Guyomar team has reported several other switching techniques. Examples include synchronized switch harvesting on inductor using magnetic rectifier (SSHI-MR) [9], Hybrid SSHI and synchronized switching and discharging to a storage capacitor through an inductor (SSDCI) [10]-[12]. All these strategies are based on the real-time identification of the resonant frequency of the vibrating structure.

In this context, to improve the extracted energy, the research study and propose the best network topology of generators positioned at different locations of the SHHI circuit, but many problems arise when deploying these non-linear energy recovery topologies [13]-[15]. They are based on signal detection, circuit frequencies, switch operation, optimal load. DSSH technique consists of a nonlinear treatment of the output voltage of the piezoelectric element. In addition, the advantage of this approach compared with the usual standard technique is that the extracted power is independent of the load. In this work is to propose different network topologies based on the DSSH technique to extract the maximum power independently of the adapted frequency and the resistive load of the same system without losses. Then to show the feasibility of such a network and to study the different ways of connecting the piezoelectric elements while using the technique of improving DSSH energy extraction. The case of a multi-mode plate structure excited in pulse mode is considered. Finally, the different network topologies will be described. The harvesting capacities of the different network topologies will be presented and compared. The goals of the next sections are to present and use a theoretical model and simulation results to demonstrate the DSSH technique preformance coupling with the piezoelectric materials for mechanical energy harvesting applications.

2. THEORETICAL ANALYSIS AND SYSTEM DESIGN

2.1. System design

The electromechanical behavior of the generator is studied from simplified way. Indeed, around the resonant frequency of the structure, and in the case of a small displacement for which the movement remains linear, the piezoelectric generator can be modeled by a "mass+piezo+spring+damper" [16]. In addition, the piezoelectric element is coupled to a host structure. A simple but representative modeling (close to the resonances) of such a system is a simple second order, as illustrated by Figure 1 and which follows a behavior described by relation (1), where u, F, V, and I respectively represent the displacement at a point of the structure, the applied force, the voltage and the current leaving the active element.

A multimodal Mass-Spring-Damper model is used to describe the whole structure in Figure 2. Considering an m mode system with n piezoelectric patches, the mechanical equations can be written for each model. The governing equation of M_m mode and nth piezoelectric patch are given in (1).

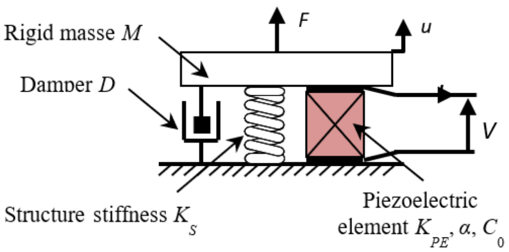

Figure 1. Mechanical representation of the piezoelectric systems

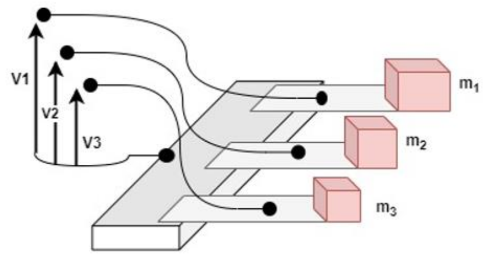

Figure 2. The structure of piezoelectric energy harvester array

The equations of the electromechanical behavior of an intelligent structure [4]:

$$M_m\ddot{u}_m + C_m\dot{u}_m + K_m^E u_m = -\sum_{j=1}^{n} a_{ij}V_j + \beta_m F \quad (1)$$

$$I_n = \sum_{k=1}^{m} a_{kn}\dot{u}_k - C_{0n}\dot{V}_n \quad (1)$$

M_m, C_m and K_m are then defined respectively as the dynamic mass, the structural damping factor and the short-circuit stiffness. α and C_0 are respectively the equivalent force factor and the equivalent blocked capacitance of the piezoelectric insert. From (1), we can establish an electrical diagram generator equivalent. The electrical part is separate of the mechanical part by a perfect transformer with gain α. By analogy, in the mechanical branch, the equivalent stiffness K_m is represented by a capacitor C_m, the mass M_m by an inductance L_m and the damping D by a resistance R_m.

2.2. Double synchronized switch harvesting (DSSH)

The research developed the double synchronized switch harvesting (DSSH) consists of a combination of the serial SSHI and SECE architectures, as shown in Figure 3 [6], [9]. This technique control between voltage increase and energy recovery. In addition, the DSSH technique allows recovered power independent of the load. In the case of constant amplitude excitation at the resonant frequency, it has been shown that this technique also extracts energy much faster than all other techniques [8]. This configuration is controlled differently from the parallel SSHI configuration. Switch S_2 is closed only when C_{int} is fully charged by the rectifier, while switch S_1 is closed only when the energy stored in L_2 is maximum.

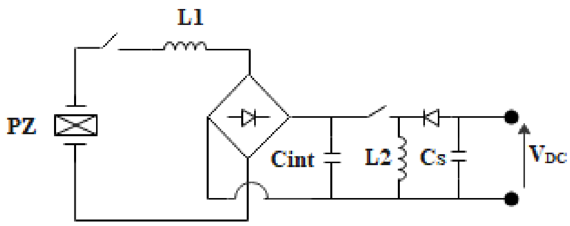

Figure 3. Piezoelectric energy harvesting system with DSSH technique

The Mathematical expressions for DSSH circuit is subdivided into two steps as follow:

- **Step 1**: Switch S_1 is closed in the first step the current flowing through the circuit when the switch S_1 is closed and we find in (2).

$$u_L + u_p + u_{int} = 0$$

$$L_1\ddot{q}_p + r_1\dot{q}_p + \frac{q_p}{C_{eq}} = 0 \quad (2)$$

$$C_{eq} = \frac{C_{pz}C_{int}}{C_{pz}+C_{int}} \quad (3)$$

Where:

$C_{eq:}$: the equilavent capacitance of C_{pz} and Cint, for independent DSSH circuit
q : the piezoelectric element charge
L_1 : the series inductor connected to the piezoelement
r_1 : the internal resistance of the inductor L_1
C_{pz} : is equivalent piezoelectric capacitance
C_{int} : is Intermediate capacitance of the external circuit

The switch S_1 is opened when the voltage V_p of the piezoelectric element is maximum at its edges, the current flowing in the first part of the circuit is given by solving the second-order differential equation given in (4),

$$i_p = \dot{q}_p = C_{eq} V_p \frac{\omega_0}{\sqrt{1-\xi_0^2}} e^{-\omega_0 \xi_0 t} \sin(\omega_0 \sqrt{1-\xi_0^2}\, t) \tag{4}$$

for the switching event, with ω_o and ξ_0, the natural angular frequency and the system damping coefficient, respectively, defined as (5),

$$\omega_0 = \sqrt{\frac{1}{L_1 \frac{C_{pz}C_{int}}{C_{pz}+C_{int}}}}\, ; \xi_0 = \frac{1}{2} r_1 \sqrt{\frac{\frac{C_{pz}C_{int}}{C_{pz}+C_{int}}}{L_1}} \tag{5}$$

after this development, we deduce the expression of the energy extracted during this switching period for the independent DSSH circuit and also for the other network topology,

$$E_1 = \frac{1}{2} C_{int} \left(V_{C_{int}}\right)_{end}^2 = \frac{1}{2} C_{int} \left[\frac{C_0}{C_{int}+C_0}\ (1+\gamma_0) V_0\right]^2 \tag{6}$$

after this energy transfer process, switch S_1 gets opened and the next energy transfer process starts from intermediate capacitor to the boost inductor.

- **Step 2**: in the second part when switch S_2 is closed, the intermediate capacitor is connected to the inductor. The current flowing in the intermediate stage of the circuit is given by solving the second order differential as shown in (7).

$$i_{int} = C_{int} V_{int} \frac{\omega_{int}}{\sqrt{1-\xi_{int}^2}} e^{-\omega_{int}\xi_{int} t} sin\left(\omega_{int} \sqrt{1-\xi_{int}^2} t\right) \tag{7}$$

Where:

$$\omega_{int} = \sqrt{\frac{1}{L_2 C_{int}}} \tag{8}$$

$$\xi_{int} = \frac{1}{2} r_2 \sqrt{\frac{C_{int}}{L_2}} \tag{9}$$

the equation of the current at the end of this process is given by (10),

$$(\dot{q}_{int})_{end} \approx C_{int} (\mathrm{V}c_{int})_{end} \omega_{int} e^{-\xi_{int}\pi/2} \tag{10}$$

the expression of the harvested energy for a single operation cycle is given by (11),

$$E_{DHHS-ind} = \int V_{DC}\, \dot{q}_s dt = V_{DC} \Delta q_s \tag{11}$$

otherwise:

$$(E_2)_{DSSH-ind} = \frac{1}{2} \gamma_c C_{int} \left(V_{C_{int}}\right)_{end}^2 \tag{12}$$

with γ_C, the overall efficiency of the converter, given by,

$$\gamma_c = e^{-\xi_{int}\pi} \tag{13}$$

in the case of topology DSSH-ind, as there are multiple output capacitances ($C_{s1}=C_{s2}=C_{s3}\ldots$), the harvested energy is expressed as (14).

$$E_{DSSH_{ind}} = \sum_{j=1}^{n}\left(\frac{1}{2}\gamma_c C_{int}\left(V_{C_{int}}\right)^2_{end}\right)_j = \sum_{j=1}^{n}\left(\frac{1}{2}\gamma_c C_{int}\left(\frac{C_0}{C_{int}+C_0}(1+\gamma_0)\,V_0\right)^2_{end}\right)_j \tag{14}$$

2.3. Network topology design

In this section we will presented five networks topologies, all of them are based on the circuit DSSH and standard circuit (STD). Which includes a rectifier bridge and a storage capacitor, or the DSSH technique in Figure 4. The technique used in this work is, in fact, the DSSH. It consists of a piezoelectric element, a series inductor with small internal resistance, a diode bridge, an intermediate capacitor, and an inductor. This inductor also has small internal resistance. The circuit also has a diode, a smoothing capacitor connected to the load. There are two switches in the circuit. One switch is connected between the piezoelectric element and the uncontrolled bridge and the second switch is connected between the intermediate capacitor and the other inductance [17], [18].

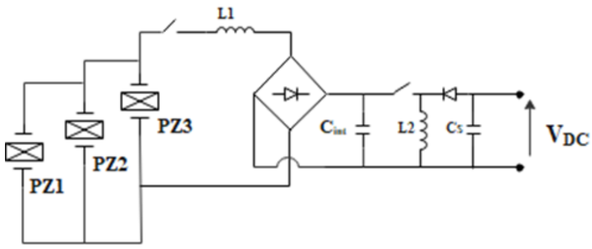

Figure 4. The circuit Mono-DSSH network

3. ENERGY HARVESTING: ANALYSIS AND PERFORMANCE STUDY

In this sub-section, the aim of this work is to analyse agile approaches to optimize the produced power by a piezoelectric generator. In order to maximize the electric energy, a performance study of the different network topologies in different places of a structure is conducted, for extract the maximum power independently of the adapted frequency and the resistive load of the same system without losses. in addition to show the feasibility of such a network and to study the different ways of connecting the piezoelectric elements while using the technique of improving DSSH energy extraction.

3.1. Energy harvesting by topology Mono-DSSH (m-D)

In network topology mono-DSSH, we connect n piezoelectric in parallel in the same circuit. The current flowing through the closed loop circuit is calculated as shown in [19], [20],

$$L_1\ddot{q}_{m-D} + r_1\dot{q}_{m-D} + \frac{q_{m-D}}{\frac{nC_0C_{int}}{nC_0+C_{int}}} = 0 \tag{15}$$

where, n is the number of piezoelectric elements. In addition, the current i_{m-D} can be expressed as,

$$i = \frac{nC_0C_{int}}{C_0+nC_{int}}\,V_0\,\frac{\omega_{m-D}}{\sqrt{1-\xi_{m-D}^2}}\,e^{-wt}\sin\left(\omega_{m-D}\sqrt{1-\xi_{m-D}^2 t}\right) \tag{16}$$

where,

$$\omega_{m-D} = \sqrt{\frac{1}{L_1\frac{nC_0C_{int}}{nC_0+C_{int}}}} \tag{17}$$

$$\xi_{m-D} = \frac{1}{2} r \sqrt{\frac{\frac{nC_0C_{int}}{nC_0+C_{int}}}{L_1}} = \frac{1}{2} \mathrm{r} \sqrt{\frac{1}{\mathrm{L}_1} \times \frac{\mathrm{C}_0\mathrm{C}_{\mathrm{int}}}{\mathrm{C}_0+\mathrm{C}_{\mathrm{int}}} \times \frac{\mathrm{n}(\mathrm{C}_0+\mathrm{C}_{\mathrm{int}})}{\mathrm{nC}_0+\mathrm{C}_{\mathrm{int}}}} = \xi_0 \sqrt{\frac{n(C_0+C_{int})}{nC_0+C_{int}}} \tag{18}$$

this first switching event stops when the current $q_{DSSH-mono}$ is null, thus giving the amount of transferred charge,

$$\Delta q_{m-D} = -\frac{nC_0C_{int}}{nC_0+C_{int}} (1+\gamma_{D-m}) V_0 \tag{19}$$

where, $\gamma_{mono-DSSH}$, the inversion factor, defined as (20),

$$\gamma_{mono-DSSH} = e^{-\pi\xi_{D-m}/\sqrt{1-\xi_{m-D}^2}} \tag{20}$$

substituting in (18) into (20) gives,

$$\gamma_{m-D} = \left(e^{-\pi\xi_0/\sqrt{1-\xi_0^2}}\right)^{\sqrt{\frac{\frac{n(C_0+C_{int})}{nC_0+C_{int}} \times (1-\xi_0^2)}{(1-\xi_0^2 \times \frac{n(C_0+C_{int})}{nC_0+C_{int}})}}} = (\gamma_0)^{\sqrt{\frac{n(C_0+C_{int}) \times (1-\xi_0^2)}{(nC_0+C_{int}) - \xi_0^2 \times n(C_0+C_{int}))}}}$$

$$= (\gamma_0)^{\sqrt{\frac{n(C_0+C_{int}) \times (1-\xi_0^2)}{n(C_0+C_{int})(1-\xi_0^2) - (n-1)C_{int}}}}$$

$$\gamma_{m-D} = (\gamma_0)^{\sqrt{\frac{1}{1-\frac{(n-1)C_{int}}{n(C_0+C_{int}) \times (1-\xi_0^2)}}}} = (\gamma_0)^{\sqrt{\frac{1}{1-\beta}}}$$

where,

$$\boldsymbol{\beta = \frac{(n-1)C_{int}}{n(C_0+C_{int}) \times (1-\xi_0^2)}} \tag{21}$$

where n the number of piezoelectric.

$$(\mathrm{V}c_{int})_{end} = \frac{nC_0}{C_{int}+nC_0} \left(1 + (\gamma_0)^{\sqrt{\frac{1}{1-\beta}}}\right) V_0 \tag{22}$$

Thus, the extracted energy for a single switch event is given by (23),

$$(E_1)_{m-D} = \frac{1}{2} C_{int} \left(V_{C_{int}}\right)_{end}^2 = \frac{1}{2} C_{int} \left[\frac{nC_0}{C_{int}+nC_0} \left(1 + (\gamma_0)^{\sqrt{\frac{1}{1-\beta}}}\right) V_0\right]^2 \tag{23}$$

during this second step, the governing equation of the current qin through the inductor L_2 is given by (24),

$$L_2\ddot{q}_{int} + r_2\dot{q}_{int} + \frac{q_{int}}{C_{int}} = 0 \tag{24}$$

yielding the expression of the current in the inductor:

$$(\dot{q}_{int})_{end} \approx C_{int} (\mathrm{V}c_{int})_{end} \omega_{int} e^{-\xi_{int}\pi/2} \tag{25}$$

where:

$$\omega_{int} = \sqrt{\frac{1}{L_2C_{int}}} \tag{26}$$

$$\xi_{int} = \frac{1}{2} r_2 \sqrt{\frac{C_{int}}{L_2}} \tag{27}$$

the harvested energy expression for a single operation cycle is given by (28),

$$(E_2)_{m-D} = \frac{1}{2}\gamma_c C_{int} \left(V_{C_{int}}\right)^2_{end} \tag{28}$$

substituting in (22) into (28) gives:

$$(E_2)_{m-D} = \frac{1}{2}\gamma_c C_{int} \left(\frac{nC_0}{C_{int} + nC_0} \left(1 + (\gamma_0)^{\sqrt{\frac{1}{1-\beta}}}\right) V_0 \right)^2_{end}$$

$$= \left(n \left(\frac{C_{int} + C_0}{C_{int} + nC_0} \right) \left(\frac{1 + (\gamma_0)^{\sqrt{\frac{1}{1-\beta}}}}{1 + \gamma_0} \right) \right)^2 \times (E_2)_{DSSH-ind}$$

3.2. Energy harvesting by topology DSSH-parallel

Expression of the energy of the network topology parallel, when C_{pz} is constant, thus the electric I_{pz} current too. Moreover, in this case we consider V_{DC} unchanged [21]-[24].

$$E_{DSSH-parallel} = \int V_{DC}\, \dot{q}_t dt = (\nabla q)_t V_{DC} \tag{29}$$

where

$$(\nabla q)_t = C_r V_{DC}; \quad (C_r)_{eq} = C_s // C_s // C_s \dots C_s = C_s + \dots + C_s = nC_s\,; \quad C_s = \frac{\Delta q_s}{V_{int}} \tag{30}$$

$$E_{DSSH-parallel} = \frac{1}{2} nC_s (V_{DC})^2 = n \frac{\Delta q_s}{V_{in}} (V_{DC})^2 \tag{31}$$

$$E_{DSSH-parallel} = \frac{1}{2} nC_{in} V_{DC} V_{int} \gamma_c = n \frac{V_{DC}}{V_{int}} \times E_{DSSH-ind}$$

3.3. Energy harvesting by topology DSSH-serie

Expression of the energy of the network topology series [24]-[26]:

$$E_{DSSH-serie} = \int V_{DC}\, \dot{q}_t dt = (\nabla q)_t V_{DC} \tag{32}$$

where

$$(\nabla q)_t = C_r V_{DC}\ ;\ (C_r)_{eq} = \frac{C_s}{n}\,;\ C_s = \frac{\Delta q_s}{V_{int}} \tag{33}$$

$$E_{DSSH-series} = \frac{1}{n} C_{in} (V_{DC})^2 \gamma_c = \frac{1}{n} \frac{(V_{DC})^2}{(V_{int})^2} \times E_{DSSH-ind} \tag{34}$$

3.4. Energy harvesting by topology parallel of the standard circuit

In the previous study [27]-[30]. at resonance frequency we discover DSSH can enhance the energy output stage. However, The DSSH methods show off higher harvesting capacity with load-independent behaviour. The harvesting capability of DSSH is decided with the aid of γ_C , the intermediate inversion issue usually decided through C_{int} and L_2, of this nonlinear circuit topology exhibit enhancement harvested energy in contrast to standard technique. The gain is around 500% percentage for DSSH circuit.

$$E_{DSSH-ind} \approx 5\, E_{STD} \tag{35}$$

For n piezoelectric:

$$E_{STD} = \frac{1}{5} \sum_{j=1}^{n} \left(E_{DSSH-ind}\right)_j \tag{36}$$

According to different expressions in Table 1 of energy for each network topologies. It has noticed that the tonic energy is being different to each topologies that is contains 3 piezoelectric. Using STD technique to compare the topologies based on circuit-DSSH, as well as STD has different energy when we want to change topologies. In this study, the authors compare STD-parallel topologies, which provides a maximal energy.

Table 1. Is significantly different from the expression energy for network topology DSSH

Energy	Expression	In function $E_{DSSH-ind}$
$E_{DSSH-ind}$	$\sum_{j=1}^{n}\left(\frac{1}{2}\gamma_c C_{int}\left(V_{C_{int}}\right)^2_{end}\right)_j$	$\sum_{j=1}^{n}(E_{DSSH-ind})_j$
$E_{DSSH-parallel}$	$\frac{1}{2}nC_{in}V_{DC}V_{int}\gamma_c$	$n\frac{V_{DC}}{V_{int}}\times E_{DSSH-ind}$
$E_{DSSH-serie}$	$\frac{1}{2n}C_{in}V_{DC}V_{int}\gamma_c$	$\frac{1}{n}\left(\frac{V_{DC}}{V_{int}}\right)^2\times E_{DSSH-ind}$
$E_{mono-DSSH}$	$\frac{1}{2}\gamma_c C_{int}\left(\frac{nC_0}{C_{int}+nC_0}\left(1+(\gamma_0)^{\sqrt{\frac{1}{1-\beta}}}\right)V_0\right)^2_{end}$	$\left(n\left(\frac{C_{int}+C_0}{C_{int}+nC_0}\right)\left(\frac{1+(\gamma_0)^{\sqrt{\frac{1}{1-\beta}}}}{1+\gamma_0}\right)\right)^2\times(E_2)_{DSSH-ind}$
E_{STD}	$\frac{1}{5}\sum_{j=1}^{n}\left(\frac{1}{2}\gamma_c C_{int}\left(V_{C_{int}}\right)^2_{end}\right)_j$	$\sum_{j=1}^{n}\left(\frac{1}{5}E_{DSSH-ind}\right)_j$

In Figure 5 we have a system contains 3 piezoelectric samples based on different forms, mainly we have got that the harvested energies which is used in the topologies Mono-DSSH is essentially important and it's little bit more than DSSH-parallel nearly 120%. We have also found that mono-DSSH is more than DSSH-series composition by 650% and it has exceed DSSH-ind by 240%. In this part of work, the authors studied the influence of change the piezoelectric samples number. The second Figure 6, a changing to energy of the number n. We have noticed increasing of the standard energy, which divides into 3 cases. In the first case when n≤4 we find that the standard energy is maximum in the composition DSSH-mono comparing to other compositions. When n=4 energy becomes DSSH-mono and DSSH-parallel maximal and nearly equal. In this case, DSSH-mono composition stays easy and weak in the process. Also economical to wasted energy on the level of electronic elements, the rate of dissipation highly increases too. In the case of n>4, we have noticed that the curve of extracted energy in DSSH-parallel composition is important to other composition and it has multiplied when piezo quantity increased. Finally, we can get maximal energy from forms which contain energy resources "piezoelectric materials" by standing on DSSH-mono composition when n≤4 and including DSSH-mono composition method and DSSH- parallel when piezo is more than 4 piezoelectrics samples.

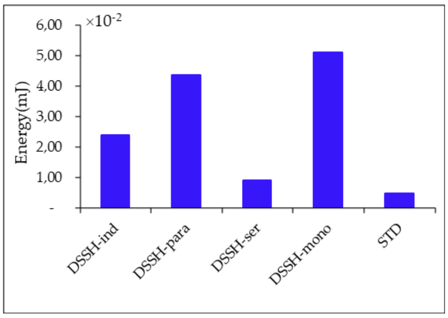

Figure 5. The energy of different network topologies

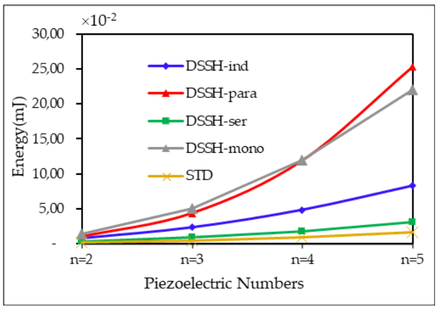

Figure 6. The energy harvested in different network topologies as a function of piezoelectric samples number

4. SIMULATION RESULTS

In this subsection, we will discuss the results of the simulation to show that the energy produced is critically dependent on how the DSSH circuits are connected. The structure that will be used in the simulations is a generator of the current I_{PZ} parallel with a capacitor C_{PZ} [31]-[33] in Figure 7. This model used in physical security information managemen (PSIM) by adding the recovery device. Its dimensions and physical properties are given in Table 2.

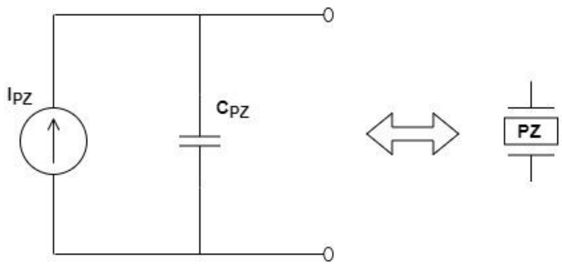

Figure 7. The equivalent circuit of a piezoelectric material

Table 2. The parameters of the piezoelement

Element	Value
Piezoelement current I_{PZ}	1 mA
Piezoelement capacitor C_{PZ}	30 nF
Resonance frequency f_0	105.3 Hz
Piezoelement current I_{PZ}	1 mA

The simulation in this part shows the difference in energy recovered by the network topology studied as a function of the piezoelectric numbers. Through the Figure 8, it turns out that there are almost the same results between studying theory and simulation, so that the DSSH-parallel and Mono-DSSH topology is the best, also energy harvesting for network topology STD is negligible compared to the other topologies. When the piezo number is less than 4 we notice that the DSSH-parallel and Mono-DSSH topologies have approximately the same results, while in the case of n<4, we find that the DSSH-parallel structure is better compared to the Mono-DSSH. It explains the difference in energy extraction between the DSSH-parallel and Mono-DSSH topology, until we find that the mono DSSH structure is better, due to the presence of a limited number of electronic components and thus less energy when the piezoelectric number is less than 4. On the other hand, in the case of n>4, we find that the DSSH-parallel structure is better and the higher the piezo number and the energy loss remains limited, during Mono-DSSH installation, more power is lost due to higher current in the electronic components.

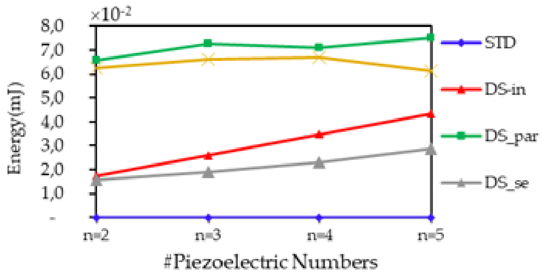

Figure 8. The energy of different network topologies as a function of piezoelectric number

5. CONCLUSION

In the embedded systems study network topology circuit is very important for to extract maximum energy. In this work, the authors are studied a five networks topologies for piezoelectric energy harvesting and compared the different networks topologies based on a DSSH circuit (circuit Standard, Independent DSSH, DSSH in parallel, Mono-DSSH, DSSH in series), have been in distinction in the network topology of structure damping harvested voltage, and energy. These topologies consist of non-linear DSSH bind networks in order to optimize, the extracted energy. Moreover, simulation have been conducted and results confirmed that the better network topology, finally we conclude can get maximal energy from forms which contain energy resources "piezoelectric materials" by standing on Mono-DSSH composition when n≤4 and including mono-DSSH composition method and DSSH-parallel when piezoelectric is more than 4 piezoelectric sapmles. Then we can compose each piezo 4 in circuit DSSH and the last takes DSSH-Mono in parallel.

REFERENCES

[1] D. Guyomar, A. Badel, E. Lefeuvre, and C. Richard, "Toward energy harvesting using active materials and conversion improvement by nonlinear processing," *IEEE transactions on ultrasonics, ferroelectrics, and frequency control*, vol. 52, no 4, p. 584-595, 2005, doi: 10.1109/TUFFC.2005.1428041.

[2] C. Jean-Mistral, A. Sylvestre, S. Basrour, and J. J. Chaillout, "Dielectric properties of polyacrylate thick films used in sensors and actuators," *Smart materials and structures*, vol. 19, no 7, 2010, doi: 10.1088/0964-1726/19/12/125009.

[3] E. Lefeuvre, D. Audigier, C. Richard, and D. Guyomar, "Buck-boost converter for sensorless power optimization of piezoelectric energy harvester," *IEEE Transactions on Power Electronics*, vol. 22, no 5, pp. 2018-2025, 2007, doi: 10.1109/TPEL.2007.904230.

[4] E. Lefeuvre, A. Badel, C. Richard, and D. Guyomar, "Piezoelectric energy harvesting device optimization by synchronous electric charge extraction," *J. of intell. material syst. and structures*, vol. 16, no 10, pp. 865-876, 2005, doi: 10.1177/1045389X05056859.

[5] Y. Wu, A. Badel, F. Formosa, W. Liu, and A. E. Agbossou, "Piezoelectric vibration energy harvesting by optimized synchronous electric charge extraction," *Journal of Intelligent Material Systems and Structures*, vol. 24, no 12, pp. 1445-1458, 2013, doi: 10.1177/1045389X13517315.

[6] M. Lallart, L. Garbuio, L. Petit, C. Richard, and D. Guyomar, "Double synchronized switch harvesting (DSSH): A new energy harvesting scheme for efficient energy extraction," *IEEE transactions on ultrasonics, ferroelectrics, and frequency control*, vol. 55, no 10, pp. 2119-2130, 2008, doi: 10.1109/TUFFC.912.

[7] M. Lallart, "Nonlinear technique and self-powered circuit for efficient piezoelectric energy harvesting under unloaded cases," *Energy Conversion and Management*, vol. 133, pp. 444-457, 2017, doi: 10.1016/j.enconman.2016.10.065.

[8] E. A. Squeo and F. Quadrini, "Shape memory epoxy foams by solid-state foaming," *Smart Materials and Structures*, vol. 19, no. 10, p. 105002, 2010, doi: 10.1088/0964-1726/19/11/115017.

[9] M. Lallart, C. Richard, L. Garbuio, L. Petit, and D. Guyomar, "High efficiency, wide load bandwidth piezoelectric energy scavenging by a hybrid nonlinear approach," *Sensors and Actuators A: Physical*, vol. 165, no 2, pp. 294-302, 2011, doi: 10.1016/j.sna.2010.09.022.

[10] L. Wu, P. Zhu, and M. Xie, "Self-Powered Hybrid SSHI Circuit with a Wide Operation Range for Piezoelectric Energy Harvesting," *Sensors*, vol. 21, no 2, p. 615, 2021, doi: 10.3390/s21020615.

[11] M. Lallart, W. J. Wu, L. Yan, and S. W. Hung, "Inductorless synchronized switch harvesting using a piezoelectric oscillator,". I*EEE Transactions on Power Electronics*, vol. 35, no 3, pp. 2585-2594, 2019, doi: 10.1002/eng2.12266.

[12] D. Guyomar and M. Lallart, "Recent progress in piezoelectric conversion and energy harvesting using nonlinear electronic interfaces and issues in small scale implementation," *Micromachines*, vol. 2, no 2, pp. 274-294, 2011, doi: 10.3390/mi2020274.

[13] Y. Li, D. Guyomar, and C. Richard, "Influence of the topology for a networked SSHI piezoelectric harvesting configuration," In *Active and Passive Smart Structures and Integrated Systems 2013*, 2013. p. 868808, doi: 10.1117/12.2006130.

[14] S. Chen *et al.*, "Adsorption/desorption and electrically controlled flipping of ammonia molecules on graphene," *New Journal of Physics*, vol. 12, no 12, p. 125011, 2010, doi: 10.1088/1361-665X/ab6484.

[15] A. Hajjaji *et al*., "Nonlinearity and scaling behavior in a soft lead zirconate titanate piezoceramic," *Journal of Applied Physics*, vol. 108, no 6, 2010, doi: 10.1063/1.3486510.

[16] H. Shen, J. Qiu, H. J, K. Zhu, and M. Balsi, "Enhanced synchronized switch harvesting: a new energy harvesting scheme for efficient energy extraction," *Smart Materials and Structures*, vol. 19, no 11, p. 115017, 2010, doi: 10.1088/0964-1726/19/11/115017.

[17] H. A. Sodano, G. Park, and D. J. Inman, "Estimation of electric charge output for piezoelectric energy harvesting," *Strain*, vol. 40, no 2, pp. 49-58, 2004, doi: 10.1111/j.1475-1305.2004.00120.

[18] Z. Alaei, "Power Enhancement in Piezoelectric Energy Harvesting," *DiVA*, 2016.

[19] E. Minazara, D. Vasic, F. Costa, and G. Poulin, "Piezoelectric diaphragm for vibration energy harvesting," *Ultrasonics*, vol. 44, p. e699-e703, 2006, doi:10.1016/j.ultras.2006.05.141.

[20] G. K. Ottman, H. F. Hofmann, A. C. Bhatt, and G. A. Lesieutre, "Adaptive piezoelectric energy harvesting circuit for wireless remote power supply," *IEEE Transactions on power electronics*, vol. 17, no 5, pp. 669-676, 2002, doi: 10.1109/TPEL.2002.802194.

[21] A. Rjafallah, A. Hajjaji, D. Guyomar, K. Kandoussi, F. Belhora, and Y. Boughaleb, "Modeling of polyurethane/lead zirconate titanate composites for vibration energy harvesting," *Journal of Composite Materials*, 2019, vol. 53, no 5, p. 613-623, 2019, doi: 10.1177/0021998318788604.

[22] W. W. Clark, "Vibration control with state-switched piezoelectric materials," *Journal of intelligent material systems and structures*, vol. 11, no 4, pp. 263-271, 2000, doi: 10.1106/18CE-77K4-DYMG-RKBB.

[23] A. Brenes, A. Morel, J. Juillard, E. Lefeuvre,, and A. Badel, "Maximum power point of piezoelectric energy harvesters: a review of optimality condition for electrical tuning," *Smart materials and structures,* vol. 29, no 3, 2020, doi: 10.1088/1361-665X/ab6484.

[24] A. Badel, A. Benayad, E. Lefeuvre, L. Lebrun, C. Richard, and D. Guyomar, "Single crystals and nonlinear process for outstanding vibration-powered electrical generators," *IEEE Transactions on ultrasonics, ferroelectrics, and frequency control*, vol. 53, no 4, pp. 673-684, 2006, doi: 10.1109/TUFFC.2006.1611027.

[25] J. Hong, F. Chen, M. He, S. Wang, W. Chen, and M. Guan, "Study of a low-power-consumption piezoelectric energy harvesting circuit based on synchronized switching technology," *Energies*, vol. 12, no 16, p. 3166, 2019, doi: 10.3390/en12163166.

[26] Y. Elhmamsy, C. Ennawaoui, A. Hajjaji, and Y. Boughaleb, "Theoretical study and Simulation method for optimizing the performance of advanced Energy Harvesting techniques," *IOP Conference Series: Materials Science and Engineering*, 2020, p. 012014, doi: 10.1088/1757-899X/948/1/012014.

[27] C. Ennawaoui, H. Lifi, A. Hajjaji, A. Elballouti, S. Laasri, and A. Azim, "Mathematical modeling of mass spring's system: Hybrid speed bumps application for mechanical energy harvesting," *Engineering Solid Mechanics*, vol. 7, no 1, pp. 47-58, 2019, doi: 10.5267/j.esm.2018.11.002.

[28] Y. El Hmamsy, C. Ennawaoui, I. Najihi, and A. Hajjaji, "The synchronized electrical charge extraction regulator for harvesting energy using piezoelectric materials," *International Conference on Digital Technologies and Applications*, 2021, pp. 1517-1527, doi: 10.1007/978-3-030-73882-2_138.

[29] B. Fatima, C. Mama, and B. Benaissa, "Design methodology of smart photovoltaic plant," *International Journal of Electrical and Computer Engineering (IJEECS),* vol. 11, no 6, pp. 4718-4730, 2021, doi: 10.11591/ijece.v11i6.pp4718-4730.

[30] Y. El Hmamsy, C. Ennawaoui, and A. Hajjaji, Chouaib, "Study and design the circuit for piezoelectric vibration energy harvester to charge a datalogger," *International Journal of Engineering and Applied Physics*, vol. 1, no 1, pp. 18-25, 2021, doi: 10.1016/j.synthmet.2012.08.012.

[31] M. R. Niazi *et al.*, "Solution-printed organic semiconductor blends exhibiting transport properties on par with single crystals," *Nature communications*, vol. 6, no 1, pp. 1-10, 2015, doi:10.1016/j.synthmet.2012.08.012.
[32] C. Ennawaoui *et al.*, "Piezoelectric and Electromechanical Characteristics of Porous Poly (Ethylene-co-Vinyl Acetate) Copolymer Films for Smart Sensors and Mechanical Energy Harvesting Applications," *Applied System Innovation*, vol. 4, no 3, p. 57, 2021, doi: 10.3390/asi4030057.
[33] I. Ahmad, S. Ullah, S. Ullah, W. Ullah, U. Habib, S. Khan, and J. Anguera, "Maple-Leaf Shaped Broadband Optical Nano-Antenna with Hybrid Plasmonic Feed for Nano-Photonic Applications," *Applied Sciences*, vol. 11, no 19, p. 8893, 2021, doi: 10.3390/app11198893.

BIOGRAPHIES OF AUTHORS

Youssef El Hmamsy was born in El Jadida, Morocco, on January 08, 1989. He received his master degree in microelectronics from the Ibn Toufail University in Kénitra, Morocco. Currently, he is a Ph. D. candidate in Laboratory of Engineering Sciences for Energy (LabSIPE), National School of Applied Sciences, Chouaib Doukkali University, El Jadida, Morocco. He can be contacted at email: elhmamsyyoussef@gmail.com.

Chouaib Ennawaoui was born in Morocco. He achieved an industrial engineer degree from National School of applied Sciences Marrakech in Cadi Ayyad University, 2013. He obtained his Ph. D. from National School of applied sciences El Jadida (ENSAJ) in Chouaib Doukkali University, 2019. He is currently working as Ass. professor in ENSAJ. His main research interest is functional dielectrics, mechanical characterizations, piezoelectric polar polymer films and polymer foams, 3D/4D printed polymers, and their applications. He can be contacted at email: chouaib.enna@gmail.comy.

Abdelowahed Hajjaji was born in Morocco. He received his master's degree in materials sciences from National Institute for Applied Sciences, Lyon, France, in 2004 and his Ph. D. degree in Materials Behaviors, Vibration Control and Energy Harvesting in 2007. He obtained his habilitation from National School of Applied Sciences (ENSAJ), El Jadida, Morocco in 2014. He is currently head of Laboratory of Engineering Sciences for Energy at Chouaib Doukkali University. His current research activities include piezoelectric systems, energy harvesting, vibration control, and noise reduction. He can be contacted at email: hajjaji.a@ucd.ac.ma.